Basic and Clinical
NEUROSCIENCE
March & April 2026, Vol 17, No. 2

Research Paper

Neurotoxicity of Alginate-coated Silver Nanostructures in the Mouse Cerebellum: Acute and Chronic Effects

Mahsa Nazari[1], Ronak Shabani[2], Maryam Akhavan Tavakoli[3], Asghar Marzban[4], Sahar Eghbali[5], Rana Mehdizadeh[6], Sahar Hakimpour[7], Mehdi Mehdizadeh[2*]

1. Department of Anatomy and Pathology, School of Medicine, Shahed University, Tehran, Iran.
2. Department of Anatomy, Reproductive Sciences and Technology Research Center, School of Medicine, Iran University of Medical Sciences, Tehran, Iran.
3. Department of Anatomical Sciences, Cognitive Neurosciences, TeMS.C., Islamic Azad University, Tehran, Iran.
4. Department of Pediatrics, School of Medicine, Zanjan University of Medical Sciences, Zanjan, Iran.
5. Department of Anatomy, School of Medicine, Iran University of Medical Sciences, Tehran, Iran.
6. School of Dentistry, CT.C., Islamic Azad University, Tehran, Iran.
7. Department of Physiology, School of Veterinary Medicine, Shiraz University, Shiraz, Iran.

Use your device to scan and read the article online

Citation Nazari, M., Shabani, R., Akhavan Tavakoli, M., Marzban, A., Eghbali, S., & Mehdizadeh, R., et al. (2026). Neurotoxicity of Alginate-coated Silver Nanostructures in the Mouse Cerebellum: Acute and Chronic Effects. *Basic and Clinical Neuroscience, 17*(2), 295-308.

http://dx.doi.org/10.32598/bcn.17.2.8379.1

Article info:
Received: 30 Sep 2025
First Revision: 18 Nov 2025
Accepted: 08 Feb 2026
Available Online: 01 Mar 2026

Keywords:
Silver nanostructures (Ag-NS), Neurotoxicity, Cerebellum, Apoptosis, Autophagy, Alginate coating

ABSTRACT

Introduction: Silver nanoparticles (AgNPs) have been shown to cross the blood–brain barrier (BBB) and induce neurotoxicity. In light of the widespread application of silver nanoparticles in industrial and medical fields, this study aimed to investigate the cerebellar toxicity of a newly developed silver nanostructure (alginate-coated silver nanostructures [Ag-NS]), focusing on their physicochemical characteristics and biological impact following acute and chronic exposure.

Methods: Au@Ag core–shell nanorods were synthesized and characterized. Forty male mice were randomly divided into five groups: a control group, two sham groups (administered alginate solution at 1.5 mg/kg/day for 14 and 35 days), and two treatment groups (administered Ag-NS at the same dose and durations). Cerebellar tissue was collected and analyzed for DNA fragmentation using the TUNEL assay. Gene expression levels of apoptotic (*Bax*, *Bcl-2*, and *Caspase-3*) and autophagy-related (*LC3* and *Beclin-1*) genes were quantified using real-time PCR. Neuronal morphology was assessed via cresyl violet staining.

Results: High-resolution transmission electron microscopy (HR-TEM) analysis confirmed that the nanostructures were uniform, rod-shaped particles averaging approximately 60 nm in length. TUNEL staining revealed a significant increase in DNA fragmentation in Ag-NS-treated groups. Gene expression analysis showed upregulation of apoptotic markers and downregulation of autophagy-related genes. Histological examination revealed a marked increase in degenerated Purkinje cells (dark cells) in the treatment groups.

Conclusion: Exposure to alginate-coated Au@Ag nanorods induced significant cerebellar toxicity, particularly following chronic treatment, as evidenced by enhanced apoptosis and suppressed autophagy. These findings underscore the need for further studies to assess the safety of such nanostructures and optimize their design to minimize neurotoxic effects.

*** Corresponding Author:**
Mehdi Mehdizadeh, Professor.
Address: *Department of Anatomy, Reproductive Sciences and Technology Research Center, School of Medicine, Iran University of Medical Sciences, Tehran, Iran.*
Tel: *+98 (21) 86704543*
E-mail: *Mehdizadeh.m@iums.ac.ir*

Highlights

- Alginate-coated Au@Ag core–shell nanorods increased DNA fragmentation in exposed groups.
- The nanorods activated apoptosis-related pathways in exposed animals.
- Exposure increased the number of degenerating cells, including dark Purkinje cells.

Plain Language Summary

Silver-containing nanostructures are increasingly used in medicine, consumer products, and industry because of their unique physicochemical properties. However, these particles may cross the blood–brain barrier (BBB), raising concerns about their potential effects on the nervous system. In this study, we investigated whether alginate-coated Au@Ag core–shell nanorods could damage the cerebellum, the brain region responsible for balance and movement coordination. Male mice were exposed to the nanorods for either 14 or 35 days. Cerebellar tissue was then examined for DNA fragmentation, changes in the expression of genes associated with apoptosis and autophagy, and structural alterations in neurons. Exposure to the nanorods increased DNA fragmentation and the expression of apoptosis-related genes while decreasing the expression of genes involved in autophagy, a natural process through which cells remove damaged components and maintain cellular integrity. Histopathological examination also revealed an increased number of degenerating Purkinje cells, including dark cells. Purkinje cells are essential neurons involved in cerebellar function. These adverse effects were more pronounced following prolonged exposure. These findings suggest that alginate-coated Au@Ag core–shell nanorods may exert neurotoxic effects despite their potential biomedical applications. Further research is required to clarify their long-term safety and support the development of safer nanomaterials with reduced neurotoxic potential.

Introduction

Metal-based nanoparticles, especially silver nanoparticles (AgNPs), have attracted significant interest in nanomedicine due to their unique physicochemical and biological properties, such as antimicrobial, anticancer, and catalytic activities (Sánchez-López et al., 2020; Sofi et al., 2021). AgNPs are widely incorporated into commercial and medical products, including wound dressings, cosmetics, food packaging, dental materials, and drug delivery systems (Ahmed et al., 2017; Thakur et al., 2014). However, growing evidence indicates that AgNPs pose potential health risks, as exposure through inhalation, ingestion, dermal absorption, or intravenous routes can lead to their accumulation in organs, like the liver, spleen, kidneys, and brain (Ahmed et al., 2017; Demir, 2021; Wei et al., 2015). Their toxicity is primarily linked to oxidative stress, ionic silver (Ag^+) release, mitochondrial dysfunction, and apoptosis induction (Demir, 2021; Dos Santos et al., 2014). Anisotropic AgNPs, such as nanorods, display improved physical properties over spherical particles; however, their biocompatibility requires thorough evaluation (Durairaj et al., 2019). Coating strategies using polymers, like sodium alginate can enhance stability and minimize toxicity by modulating surface reactivity (Demir, 2021).

Critically, AgNPs can penetrate the blood–brain barrier (BBB) through passive diffusion or endocytic pathways, leading to accumulation within the central nervous system (CNS) (Ghooshchian et al., 2017; Hoet et al., 2004; Trickler et al., 2010). AgNP-induced neurotoxicity has been attributed to inflammation, BBB disruption, and direct damage to neurons and glial cells. The extent of toxicity varies with particle size, surface coating, and dosage (Mohamed et al., 2021). Previous in vivo studies in rodents have demonstrated cognitive impairments and synaptic alterations following AgNP exposure, with mechanisms implicating oxidative stress, altered gene expression, and apoptosis (Ahamed et al., 2010; Nejati et al., 2018; Yin et al., 2013). Given their ability to bypass natural biological barriers and exert neurotoxic effects, a comprehensive understanding of AgNPs' long-term impact on neural tissues is critical.

Although anisotropic AgNPs have better properties than spherical ones, it is crucial to assess the biocompatibility and toxicity of these anisotropic AgNPs (Durairaj et al., 2019). Despite numerous studies on acute exposure and spherical nanoparticles, the chronic effects of anisotro-

pic AgNPs and their underlying molecular mechanisms remain less well understood. This study investigated the acute and chronic toxicity of a novel AgNP structure—alginate-coated Au\@Ag core–shell nanorods—on the mouse cerebellum, evaluating apoptotic and autophagic markers alongside histological changes to elucidate their impact on cerebellar integrity and function.

Materials and Methods

Synthesis and characterization of silver nanostructures

As previously described (Nazari et al., 2023), gold-silver core–shell nanorods (Au@Ag) were synthesized using a seed-mediated growth method. The nanostructures were subsequently characterized to confirm morphology, size, and core–shell composition using high-resolution transmission electron microscopy (HR-TEM).

Animal groups and experimental design

Forty adult male mice (5 weeks old, 25–30 g) were obtained from the Center of Experimental and Comparative Studies at Iran University of Medical Sciences. All experimental protocols adhered to the guidelines set by the National Institutes of Health (NIH) and were approved by the Institutional Animal Ethics Committee at Iran University of Medical Sciences, Tehran, Iran.

Mice were housed under standard conditions: a 12-hour light/dark cycle at a temperature of 22–25 ˚C with unrestricted access to food and water. Animals were randomly assigned to five experimental groups (n=8 per group):

Control group: No treatment.

Sham group 1 (Al-14): Received alginate solution (1.5 mg/kg/day, intraperitoneally) (Nazari et al., 2023) for 2 weeks (Xu et al., 2015).

Sham group 2 (Al-35): Received alginate solution (1.5 mg/kg/day, intraperitoneally) for 5 weeks.

Treatment group 1 (Ag-14): Received Ag nanostructures (1.5 mg/kg/day, intraperitoneally) for 2 weeks.

Treatment group 2 (Ag-35): Received Ag nanostructures (1.5 mg/kg/day, intraperitoneally) for 5 weeks.

At the end of the treatment period, mice were deeply anesthetized using ketamine (20 mg/kg) and xylazine (0.64 mg/kg). Cardiac perfusion was performed by inserting a needle into the left ventricle and flushing with physiological saline followed by 4% paraformaldehyde to fix the tissues. The right atrium was incised to allow exsanguination. After perfusion, the head was removed and post-fixed in 4% paraformaldehyde for 24 hours. The brain was then dissected and the cerebellar tissue was separated from the whole brain. A portion was stored at −80 ˚C for quantitative real-time PCR analysis (n=3 of each group), while the remaining tissue was reserved in 10% paraformaldehyde for subsequent histological processing (n=2 for TUNEL assay and n=2 for histological analysis).

RNA isolation, cDNA synthesis, and quantitative real-time PCR

Total RNA was extracted from cerebellar tissues using TRIzol reagent (Millipore Sigma, USA) and chloroform, following the manufacturer's protocol. RNA concentration and purity were assessed with a NanoDrop spectrophotometer (Thermo Fisher Scientific, USA) using absorbance ratios at 260/280 nm.

First-strand complementary DNA (cDNA) was synthesized using a commercial cDNA synthesis kit (Fermentas, Thermo Fisher Scientific, USA). Quantitative real-time PCR (qRT-PCR) was performed using a Corbett Research qPCR system (Australia) to analyze gene expression of autophagy markers (*Beclin-1* and *LC3*) and apoptosis markers (*Bax*, *Bcl-2*, and *Caspase-3*).

The 10 µL qRT-PCR reaction mixture included:

- 5 pmol of specific forward and reverse primers
- 250 ng of cDNA template
- SYBR Green/ROX dye solution (25:1 ratio)

Expression levels were normalized to β-actin, and the $2^{-\Delta\Delta Ct}$ method was used to calculate relative expression levels (Gholipour et al., 2023; Mirsanei et al., 2023). Primer sequences are provided in Table 1.

Histological analysis and TUNEL assay

After fixation, cerebellar tissues were embedded in paraffin, sectioned at 5 µm thickness using a microtome (Didsabz DS8402, Iran), and stained with cresyl violet (Nissl stain). For each animal, 20 coronal cerebellar sections were analyzed. The entire Purkinje cell layer was evaluated for neuronal counts in a blinded manner (Akhavan Tavakoli et al., 2023; Bakhtiary et al., 2010).

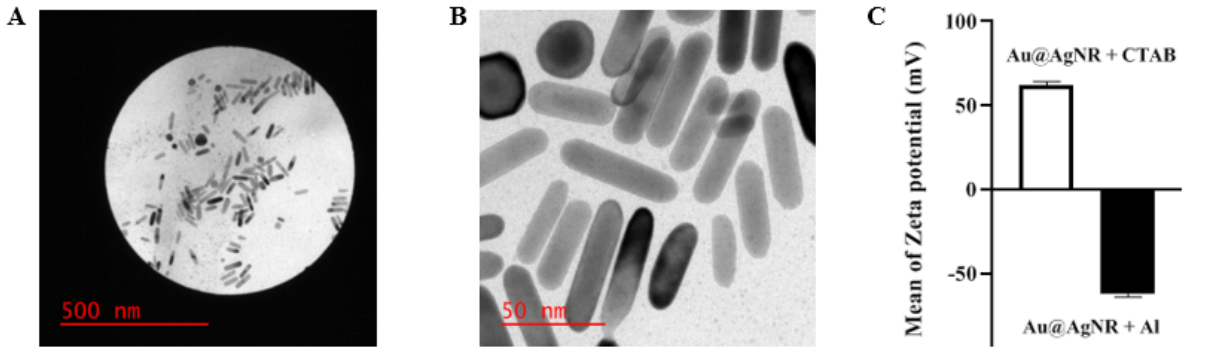

Figure 1. Characterization of silver nanostructures

A and B) High-resolution transmission electron microscopy (HR-TEM) images of Au@Ag nanorods showing uniform rod-shaped structures with core–shell morphology, C) Zeta potential measurements indicating successful coating exchange

For apoptosis detection, paraffin-embedded sections underwent deparaffinization and rehydration followed by the TUNEL assay using a commercial kit (Roche, Germany). The procedure involved:

• PBS wash (20 min, room temperature)

• Peroxidase blocking (3% H_2O_2 in methanol, 10 min)

• Permeabilization (sodium citrate/Triton X-100 solution, 15 min, 2–8 ˚C)

• Incubation with TUNEL reaction mixture (1 h, room temperature)

Propidium iodide (PI) was used for nuclear counterstaining. TUNEL-positive cells were visualized under a fluorescence microscope (Olympus, Tokyo, Japan) with a green filter at 40× magnification (Nazari et al., 2023; Pourheydar et al., 2016).

Statistical analysis

All data analyses were conducted using GraphPad Prism software, version 8. The normality of data distribution was assessed using the Kolmogorov–Smirnov test. Group comparisons and detection of significant differences between variables were performed using one-way ANOVA for gene expression data and two-way ANOVA for histological analysis. Tukey's post hoc test was subsequently applied to identify specific group differences. Data are presented as Mean±SD, with a $P<0.05$ considered indicative of statistical significance.

Results

Characterization of nanostructures

HR-TEM revealed that the synthesized Au@Ag nanostructures were rod-shaped with a uniform morphology and core–shell architecture (Figures 1A and 1B). The gold nanorod core was coated with a silver shell approximately 2.8 nm thick. The average length of the nanorods was 50–60 nm with a diameter of ~25 nm, yielding an aspect ratio of approximately 2.4. Zeta potential analysis demonstrated a substantial surface charge shift following alginate coating, with values of +62.15±1.91 mV for CTAB-coated and −62.49±1.29 mV for alginate-coated nanostructures, confirming successful surface modification (Figure 1C).

Gene expression in cerebellar tissue

Quantitative RT-PCR analysis revealed significant alterations in the expression of apoptosis- and autophagy-related genes in the cerebellum of mice treated with silver nanostructures (Figure 2). Expression of *Bax* and *Caspase-3* was significantly upregulated in both Ag 14 and Ag 35 groups compared to control and sham groups, indicating enhanced apoptotic signaling. Conversely, expression of the anti-apoptotic gene *Bcl-2* was significantly downregulated in the Ag-treated groups. Expression of *LC3*, an autophagic marker, was reduced in the treatment groups compared to the control ($P=0.0001$ and $P<0.0001$) and sham ($P=0.0002$ and $P<0.0001$) groups. Similarly, *Beclin-1* also showed downregulation in the Ag 14 and Ag 35 groups compared to the control (control vs Ag 14: $P=0.0002$; control vs Ag 35: $P=0.0003$) and sham (Al 14 vs Ag 14: $P=0.0022$; Al 14 vs Ag 35: $P=0.0033$; Al 35 vs Ag 14: $P=0.0005$; Al 35 vs Ag 35:

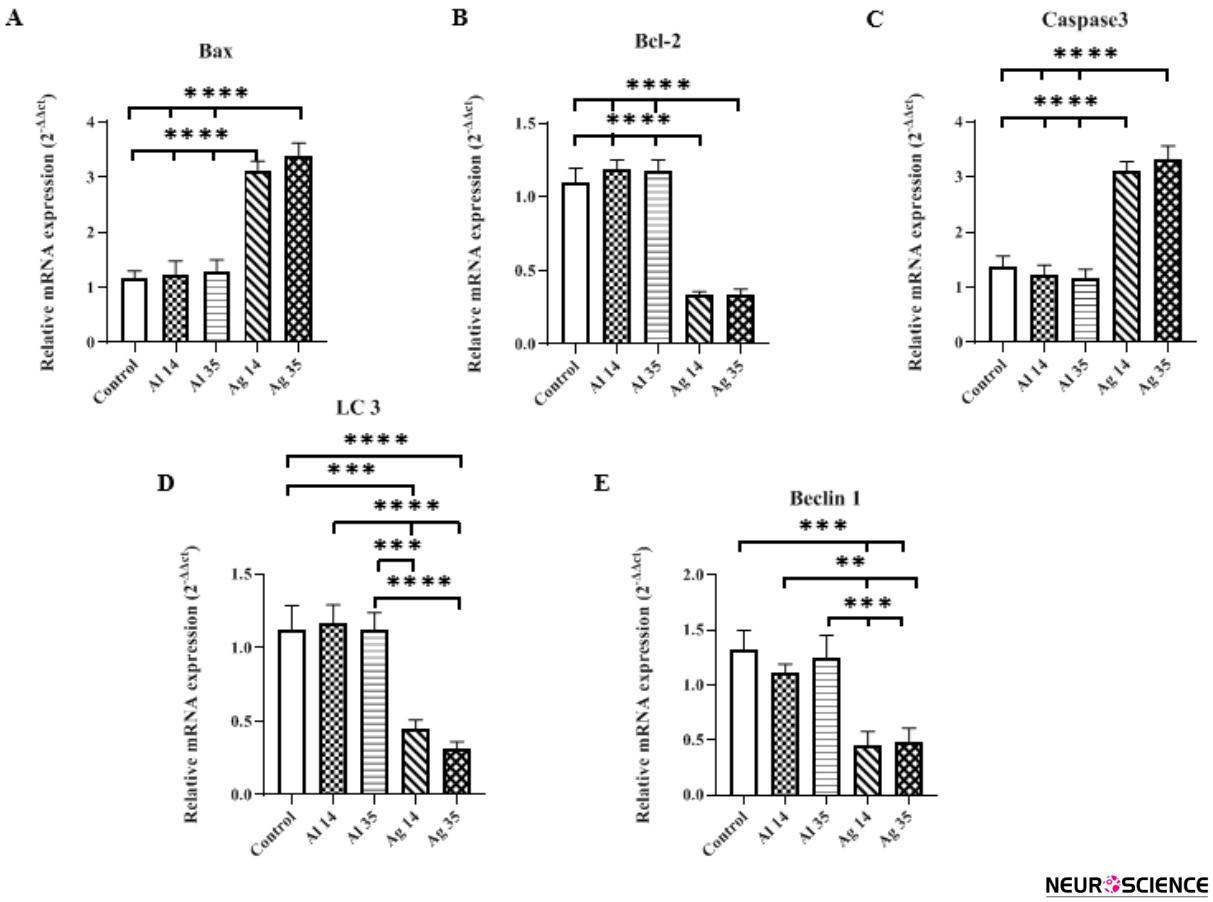

Figure 2. Expression of apoptotic and autophagy-related genes in cerebellar tissue

*P<0.05, **P<0.01, ***P<0.001, ****P<0.0001.

Note: β-actin was used as a housekeeping control. Data are presented as Mean±SD.

P=0.0007) groups. These results suggest suppression of autophagic activity in cerebellar tissue exposed to silver nanostructures. Tables 2, 3, 4, 5, and 6 present the fold-change values obtained from the qPCR analysis.

Histological analysis and TUNEL assay in cerebellar tissue

Cresyl violet (Nissl) staining identified two distinct Purkinje cell types: light cells with clearly defined nuclei and cytoplasm, representing healthy neurons, and dark cells, characterized by shrunken, basophilic cytoplasm and indistinct nuclear features, consistent with neuronal injury or degeneration (Hassanzadeh et al., 2018). A marked increase in the number of dark Purkinje cells was observed in Ag-treated groups compared to control and sham groups (P<0.0001), while the number of light cells was significantly decreased (Figures 3 and 4). Quantitative analysis revealed that the number of dark Purkinje cells significantly increased in Ag 14 (49.08±5.2) and Ag 35 (44.17±5.2) groups compared to controls. Conversely, light cell counts were significantly reduced in both treatment groups (P<0.0001).

To further confirm apoptosis, TUNEL staining was performed. Quantitative evaluation of the results showed a significant increase in TUNEL-positive nuclei (green fluorescence) in the Ag 14 (P=0.0050) and especially the Ag 35 (P=0.0019) groups, consistent with apoptotic gene expression and histopathological findings (Figures 5 and 6). Nuclei were counterstained with propidium iodide (PI, red) to facilitate visualization.

Discussion

This study explored both the acute and chronic effects of alginate-coated Au@Ag core–shell nanorods on cerebellar tissue, with particular attention to their influence on apoptotic and autophagic pathways. Treatment with these nanostructures led to a significant upregulation of pro-apoptotic genes, such as *Caspase-3* and *Bax*, along with a marked reduction in the expression of the anti-

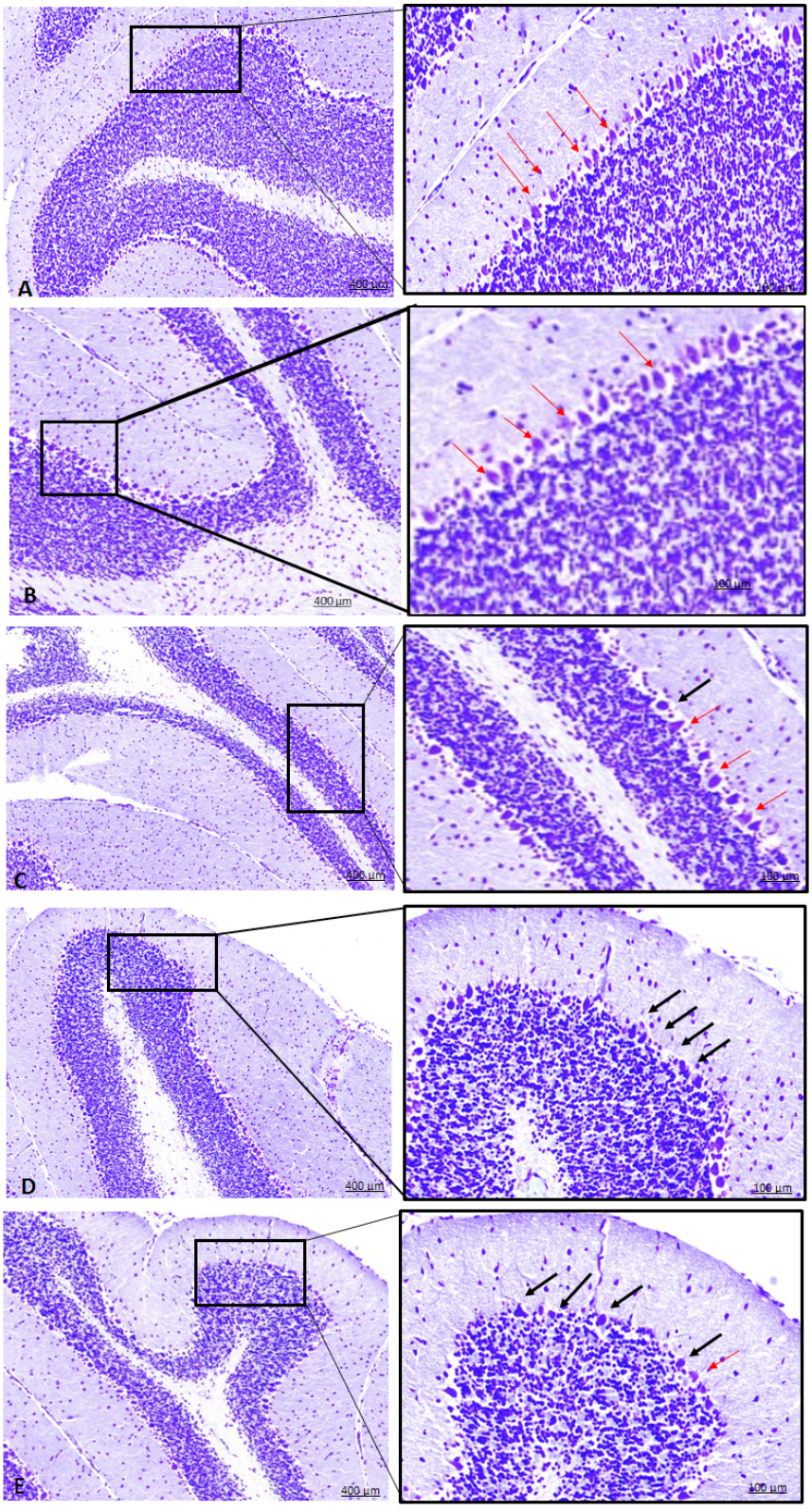

Figure 3. Nissl staining of cerebellar Purkinje cells: Representative micrographs from each group

A) Control, (B) Al 14, (C) Al 35, (D) Ag 14, and (E) Ag 35

Note: Red arrows indicate light (healthy) Purkinje cells; black arrows denote dark (degenerating) Purkinje cells. Images are shown at increasing magnification from left to right (400 µm to 100 µm).

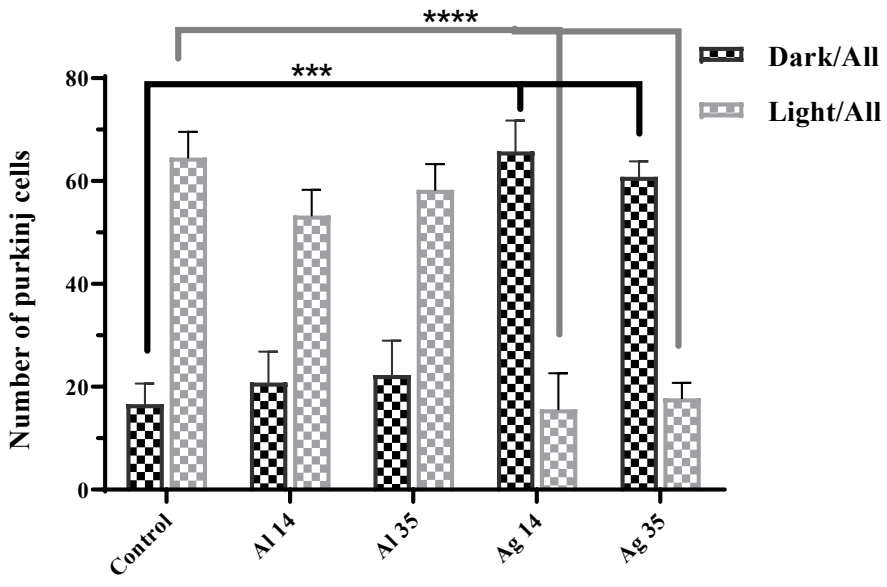

NEUROSCIENCE

Figure 4. Quantitative analysis of Purkinje cells in cerebellar sections

Note: Histogram showing a significant increase in dark Purkinje cells and a corresponding decrease in light Purkinje cells in Ag-treated groups compared to control and sham groups (***P<0.001, ****P<0.0001).

apoptotic gene *Bcl-2*. In parallel, we observed a down-regulation of autophagy-related markers, LC3 and Beclin-1, in the cerebellum of treated animals. Histological evaluation further showed an increased presence of dark Purkinje cells, a recognized indicator of neuronal injury, while TUNEL staining confirmed an increase in DNA fragmentation and apoptotic signals, particularly in the chronically exposed group. Together, these results suggest that Au@Ag nanorods disrupt cerebellar cellular

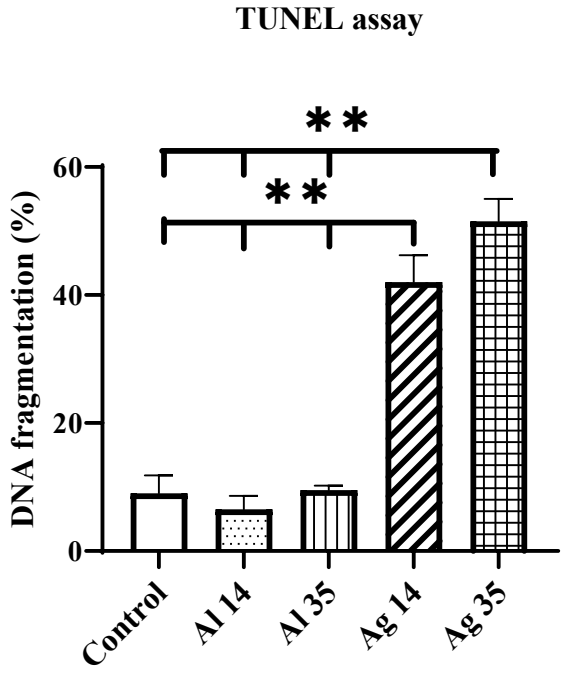

NEUROSCIENCE

Figure 5. Comparison of sperm DNA fragmentation percentage in the studied groups

Note: All results are expressed as Mean±SD (n=8); **P<0.01.

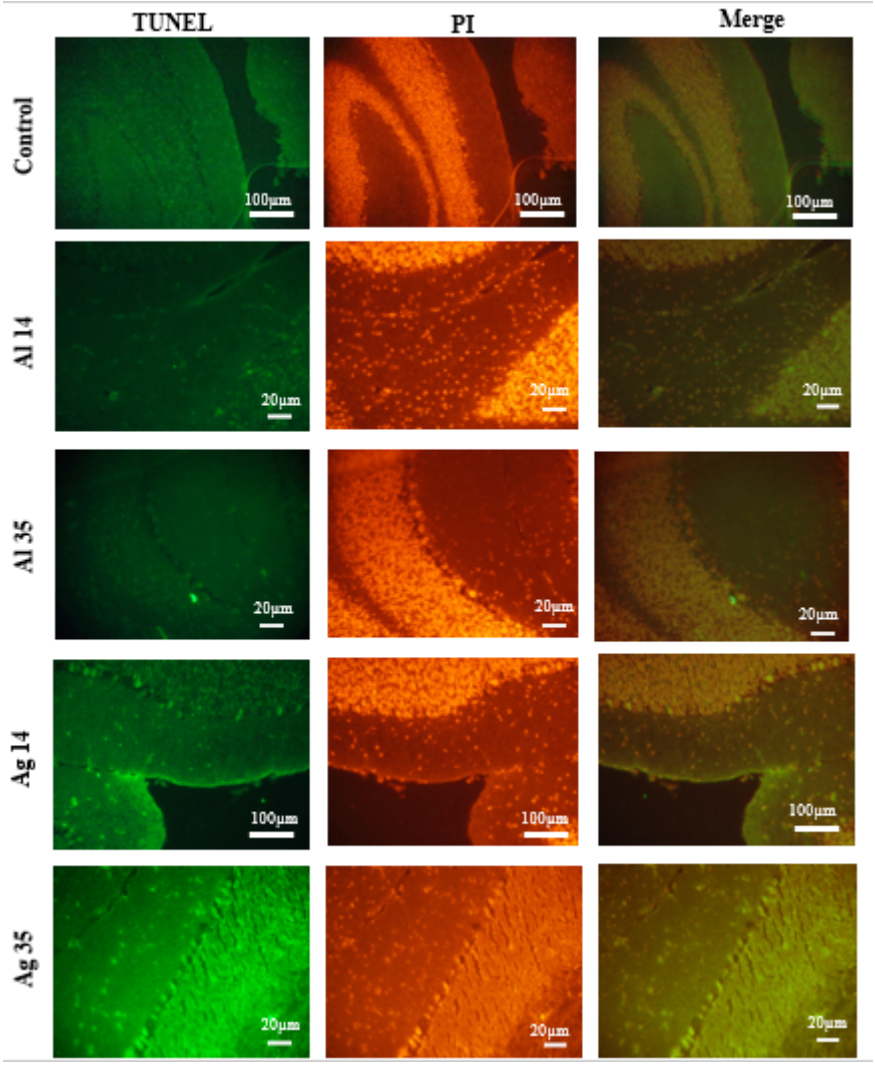

NEUROSCIENCE

Figure 6. TUNEL assay of cerebellar tissue

Note: Apoptotic cells (TUNEL-positive nuclei in green) are shown in cerebellar sections, with counterstaining by PI (red). Scale bar: 100 µm for control and Ag 14 groups; 20 µm for Al 14, Al 35, and Ag 35 groups.

homeostasis by simultaneously promoting apoptosis and impairing autophagy.

Silver is widely valued for its antimicrobial activity and high conductivity and, in its bulk form, is generally regarded as safe. However, in its ionic form (Ag^+), it becomes highly toxic, with documented effects on organisms across multiple biological systems, even at microgram-per-liter concentrations (Mertens et al., 2019). AgNPs, owing to their unique surface area and reactivity, have become prominent in various technological and medical applications. Yet, their potential for toxicity remains a critical concern. Several factors influence AgNP toxicity, including particle size, chemical composition, surface coating, concentration, duration and route of exposure, and especially their capacity to generate oxidative stress, which is widely regarded as a central mechanism of nanoparticle-induced cellular damage (Gromadzka-Ostrowska et al., 2012).

Bimetallic nanostructures, particularly those combining gold and silver in core–shell configurations, have demonstrated functional advantages, such as enhanced optical properties and biocompatibility. Gold offers structural stability and biological inertness, while silver enhances sensitivity in applications, like surface-enhanced Raman scattering (SERS) (Kvitek et al., 2020). Despite these benefits, the neurotoxicity profile of these nanostructures—especially when coated with biocompatible materials, like alginate—remains poorly understood. This study is, to our

Table 1. Primer sequences used in real-time PCR

Gene	Forward 5′–3′	Reverse 5′–3′	PCR Product Size (bp)
ß-actin	CAAGATCATTGCTCCTCCTG	ATCCACATCTGCTGGAAGG	90
Bax	AGGATGATTGCTGACGTGGA	CAAAGTAGAAGAGGGCAACCAC	118
Bcl-2	GGTGCTCTTGAGATCTCTGGTT	AGGTGGAGGAAAAATCAGGAGG	104
Caspase-3	AGGCTGACTTCCTGTATGCTT	ATGCTGCAAAGGGACTGGAT	97
Beclin-1	TTTTAGACCAGCTGGACACTCA	TGCTCACTGTCATCCTCATTCAT	106
Map1lc3b	GACGGCTTCCTGTACATGGTTT	TGGAGTCTTACACAGCCATTGC	70

NEUROSCIENCE

Table 2. Relative expression levels of Bax ($2^{-\Delta\Delta Ct}$)

Group	Replicate 1	Replicate 2	Replicate 3	Mean Fold Change	SD
Control	1.321166	1.091929	1.091503	1.168	0.108
Al 14	1.50027	1.030442	1.193945	1.241	0.238
Al 35	1.032517	1.486245	1.301573	1.273	0.227
Ag 14	3.30269	2.980039	3.105021	3.129	0.162
Ag 35	3.626465	3.163116	3.369657	3.386	0.232

NEUROSCIENCE

Note: *Bax* expression increased significantly in Ag-treated groups, indicating activation of the pro-apoptotic pathway.

knowledge, the first to evaluate the cerebellar impact of such modified Au@Ag nanorods, revealing that even with an alginate coating, significant adverse effects on neuronal integrity can occur.

Apoptosis and autophagy are essential biological processes that preserve tissue homeostasis and ensure the removal of damaged or unnecessary cells. They are tightly regulated and often interact with each other, sharing molecular regulators and signaling cascades (Nikoletopoulou et al., 2013). Apoptosis plays a key role in development and immune function, and its regulation is critically governed by proteins of the Bcl-2 family (Hon-ardoost et al., 2013; Macchi et al., 2015). These proteins include both pro-apoptotic members, such as Bax and Bak, and anti-apoptotic counterparts, like Bcl-2 and Bcl-xL (Hassan et al., 2014). Bcl-2 can prevent the release of cytochrome c from mitochondria, thus inhibiting cas-

Table 3. Relative expression levels of *Bcl-2* ($2^{-\Delta\Delta Ct}$)

Group	Replicate 1	Replicate 2	Replicate 3	Mean Fold Change	SD
Control	1.177131	0.982367	1.127386	1.096	0.099
Al 14	1.217451	1.109832	1.228497	1.185	0.064
Al 35	1.247593	1.094235	1.18413	1.175	0.077
Ag 14	0.359754	0.316528	0.330548	0.336	0.022
Ag 35	0.369216	0.298830	0.347613	0.338	0.036

NEUROSCIENCE

Note: *Bcl-2* was markedly down-regulated in Ag-treated groups, suggesting suppression of the anti-apoptotic pathway.

Table 4. Relative expression levels of *Caspase-3* ($2^{-\Delta\Delta Ct}$)

Group	Replicate 1	Replicate 2	Replicate 3	Mean Fold Change	SD
Control	1.199172	1.567249	1.375993	1.381	0.185
Al 14	1.086408	1.421444	1.176548	1.228	0.174
Al 35	0.989776	1.219112	1.295873	1.168	0.157
Ag 14	3.210122	2.908056	3.198356	3.105	0.172
Ag 35	3.028344	3.515569	3.394024	3.313	0.252

NEUROSCIENCE

Note: *Caspase-3* expression was significantly up-regulated in Ag-treated groups, confirming activation of apoptotic execution pathways.

Table 5. Relative expression levels of *LC3* ($2^{-\Delta\Delta Ct}$)

Group	Replicate 1	Replicate 2	Replicate 3	Mean Fold Change	SD
Control	1.02134	1.309046	1.051042	1.127	0.158
Al 14	1.279546	1.041758	1.190572	1.171	0.120
Al 35	0.982698	1.204778	1.169483	1.119	0.118
Ag 14	0.373304	0.499368	0.458629	0.444	0.064
Ag 35	0.360567	0.259865	0.308793	0.31	0.051

NEUROSCIENCE

Note: *LC3* expression was strongly down-regulated in Ag-treated groups, suggesting suppression of autophagy.

pase activation and cell death. Meanwhile, Beclin-1, a key autophagy regulator, is known to form a complex with Bcl-2, which can inhibit autophagic activity. During apoptosis, Beclin-1 and other autophagy-related proteins, such as Atg3 may be cleaved by caspases, linking the two processes through shared degradation pathways (Nikoletopoulou et al., 2013; Oral et al., 2012). A shift in the Bax/Bcl-2 ratio in favor of apoptosis, as seen in our study, not only promotes programmed cell death but may also suppress autophagic processes by disrupting these regulatory complexes (Aguzzi & O'connor, 2010).

The increase in dark Purkinje cells observed in Nissl-stained sections supports this conclusion, indicating structural deterioration commonly associated with oxidative or toxic stress. Additionally, the strong TUNEL positivity in Ag-treated groups confirms that DNA fragmentation—an established hallmark of apoptosis—is a major outcome of nanoparticle exposure in this model.

Table 6. Relative expression levels of *Beclin-1* ($2^{-\Delta\Delta Ct}$)

Group	Replicate 1	Replicate 2	Replicate 3	Mean Fold Change	SD
Control	1.499172	1.157249	1.310562	1.322	0.171
Al 14	1.092235	1.030456	1.194368	1.106	0.083
Al 35	1.302642	1.004759	1.410262	1.239	0.212
Ag 14	0.570076	0.467359	0.319585	0.452	0.126
Ag 35	0.453176	0.619614	0.383591	0.485	0.121

Note: *Beclin-1* expression was reduced in Ag-treated groups, indicating inhibition of autophagy initiation. NEUROSCIENCE

Taken together, the molecular, histological, and cytological data in this study provide converging evidence of cerebellar toxicity induced by prolonged exposure to alginate-coated Au@Ag nanostructures. To date, no comprehensive investigation has systematically examined the biodistribution of alginate-coated Au\@Ag core–shell nanorods within cerebellar tissue, and current studies primarily focus on spherical particles and brain regions, especially the hippocampus.

Janzadeh et al., in a meta-analysis, showed that AgNPs can induce neuronal death after crossing into the brain. Both AgNPs smaller and larger than 10 nm were capable of causing neuronal cell damage. This neurotoxic effect persisted for an extended period, lasting up to six months. Neurons from embryos of mothers exposed to AgNPs during pregnancy were similarly affected as those from animals directly exposed to the nanoparticles. Additionally, AgNP exposure was linked to impairments in memory and cognitive functions. Research suggests that inflammation and elevated oxidative stress, leading to apoptosis, are the primary mechanisms driving AgNP-induced toxicity (Janzadeh et al., 2022).

Consistent with our findings, Yin et al. conducted an in-depth investigation into the neurotoxic effects of commercially available AgNPs on rat cerebellar granule cells (CGCs) and elucidated the underlying molecular mechanisms. Their study demonstrated that AgNPs significantly compromise the viability of primary neuronal cells by inducing apoptosis associated with oxidative stress, mediated through caspase-dependent signaling pathways (Yin et al., 2013). In another study, Mohamed et al. explored the impact of AgNPs on the rat cerebellar cortex. Their findings demonstrated that exposure to Ag-NPs induced biochemical, cellular, and molecular alterations in the cerebellar cortex in a dose-dependent fashion. The primary mechanisms involved the activation of apoptotic pathways alongside increased oxidative stress and inflammation (Mohamed et al., 2020). Yin et al. also showed that exposure to AgNPs leads to cerebellar ataxia-like symptoms in rats, characterized by impaired motor coordination and reduced locomotor activity. Their results indicate that this motor dysfunction is linked to a decrease in CACNA1A expression, shedding light on the molecular mechanisms underlying AgNPs' neurotoxic effects (Yin et al., 2015).

The widespread use of AgNPs in water purification, biosensors, nasal decongestants, oral hygiene products, long-term wound dressings, and various cosmetics today represents significant risk factors for human exposure to AgNPs (Mohamed et al., 2021). Accordingly, it is suggested to investigate other shapes, structures, biocompatible coatings, and techniques to reduce the unexpected harmful effects of AgNPs in biological applications.

Challenges and limitations

Specifically, while the TUNEL assay and gene expression analyses provide valuable insights into apoptosis and autophagy, they do not capture the full complexity of molecular pathways involved in nanostructure-induced neurotoxicity. Additionally, the study is limited to male mice, which may not fully represent sex-specific responses. Furthermore, the acute and chronic exposure durations chosen may not encompass all potential exposure scenarios relevant to humans. These limitations highlight the need for further in-depth studies employing complementary techniques and diverse models to fully elucidate the neurotoxic effects of alginate-coated silver nanostructures.

Conclusion

This study demonstrates that alginate-coated Au@Ag core–shell nanorods exert toxic effects on cerebellar tissue by activating apoptotic pathways and inhibiting autophagy, particularly with prolonged exposure. Despite the use of a biocompatible alginate coating, these nanostructures induced significant neuronal degeneration and molecular alterations in the cerebellum.

Given the increasing use of AgNPs in medical and commercial products, our findings underscore the importance of further research into their long-term safety. Future studies should focus on developing strategies to reduce nanoparticle toxicity—such as optimizing particle size, dose, and surface chemistry—to ensure safe integration of these materials into biomedical applications while minimizing potential risks to neural health and human safety.

Ethical Considerations

Compliance with ethical guidelines

This study was approved by the Research Ethics Committee of Iran University of Medical Sciences (IUMS), Tehran, Iran (Code: IR.IUMS.REC.1400.1069). The experimental methodology was strictly adhered to the requirements for the use of laboratory animals and the arrive guidelines.

Funding

The present study was supported by Iran University of Medical Sciences (IUMS), Tehran, Iran (Grant No.: 1400-3-20-22370).

Authors' contributions

Conceptualization: Mahsa Nazari; Methodology: Mahsa Nazari and Ronak Shabani; Project administration: Mehdi Mehdizadeh; Investigation: Mahsa Nazari, Sahar Eghbali and Maryam Akhavan Tavakoli; Formal analysis, data curation, and data interpretation: Rana Mehdizadeh; Writing the original draft: Mahsa Nazari and Maryam Akhavan Tavakoli; Review and editing: Ronak Shabani; Final approval: Sahar Hakimpour, Ronak Shabani, and Asghar Marzban; Supervision: Asghar Marzban.

Conflict of interest

The authors declared no conflict of interest.

Acknowledgments

The experiments described in this study were conducted within the laboratories of the Anatomy Department and Cellular and Molecular Research Center (CMRC) at Iran University of Medical Sciences (IUMS), Tehran, Iran. We would like to acknowledge the support provided by the Iran University of Medical Sciences in facilitating this research.

References

Aguzzi, A., & O'Connor, T. (2010). Protein aggregation diseases: pathogenicity and therapeutic perspectives. Nature reviews. *Drug Discovery, 9*(3), 237–248. [DOI:10.1038/nrd3050] [PMID]

Ahamed, M., Posgai, R., Gorey, T. J., Nielsen, M., Hussain, S. M., & Rowe, J. J. (2010). Silver nanoparticles induced heat shock protein 70, oxidative stress and apoptosis in Drosophila melanogaster. *Toxicology and Applied Pharmacology, 242*(3), 263–269. [DOI:10.1016/j.taap.2009.10.016] [PMID]

Ahmed, S. M., Abdelrahman, S. A., & Shalaby, S. M. (2017). Evaluating the effect of silver nanoparticles on testes of adult albino rats (histological, immunohistochemical and biochemical study). *Journal of Molecular Histology, 48*(1), 9-27. [DOI:10.1007/s10735-016-9701-4] [PMID]

Akhavan Tavakoli, M., Soleimani, M., Marzban, H., Shabani, R., Moradi, F., & Ajdary, M., et al. (2023). Autophagic molecular alterations in the mouse cerebellum experimental autoimmune encephalomyelitis model following treatment with cannabidiol and fluoxetine. *Molecular Neurobiology, 60*(4), 1797-1809. [DOI:10.1007/s12035-023-03204-2] [PMID]

Bakhtiary, M., Marzban, M., Mehdizadeh, M., Joghataei, M. T., Khoei, S., & Pirhajati Mahabadi, V., et al. (2010). Comparison of transplantation of bone marrow stromal cells (BMSC) and stem cell mobilization by granulocyte colony stimulating factor after traumatic brain injury in rat. *Iranian Biomedical Journal, 14*(4), 142–149. [PMID]

Demir, E. (2021). A review on nanotoxicity and nanogenotoxicity of different shapes of nanomaterials. *Journal of Applied Toxicology, 41*(1), 118-147. [DOI:10.1002/jat.4061] [PMID]

Dos Santos, C. A., Seckler, M. M., Ingle, A. P., Gupta, I., Galdiero, S., & Galdiero, M., et al. (2014). Silver nanoparticles: Therapeutical uses, toxicity, and safety issues. *Journal of Pharmaceutical Sciences, 103*(7), 1931-44. [DOI:10.1002/jps.24001] [PMID]

Durairaj, K., Roy, B., Chandrasekaran, N., Krishnan, S. P., & Mukherjee, A. (2020). Silver nanorods induced oxidative stress and chromosomal aberrations in the Allium cepa model. *IET Nanobiotechnology, 14*(2), 161–166. [DOI:10.1049/iet-nbt.2019.0224] [PMID]

Gholipour, H., Amjadi, F. S., Zandieh, Z., Mehdizadeh, M., Ajdary, M., & Delbandi, A. A., et al. (2023). Investigation of the Effect of Seminal Plasma Exosomes from the normal and oligoasthenoteratospermic males in the implantation process. *Reports of Biochemistry & Molecular Biology, 12*(2), 294-305. [DOI:10.61186/rbmb.12.2.294] [PMID]

Ghooshchian, M., Khodarahmi, P., & Tafvizi, F. (2017). Apoptosis-mediated neurotoxicity and altered gene expression induced by silver nanoparticles. *Toxicology and Industrial Health, 33*(10), 757–764. [DOI:10.1177/0748233717719195] [PMID]

Gromadzka-Ostrowska, J., Dziendzikowska, K., Lankoff, A., Dobrzyńska, M., Instanes, C., & Brunborg, G., et al. (2012). Silver nanoparticles effects on epididymal sperm in rats. *Toxicology Letters, 214*(3), 251-258. [DOI:10.1016/j.toxlet.2012.08.028] [PMID]

Hassan, M., Watari, H., AbuAlmaaty, A., Ohba, Y., & Sakuragi, N. (2014). Apoptosis and molecular targeting therapy in cancer. *BioMed Research International, 2014,* 150845. [DOI:10.1155/2014/150845] [PMID]

Hassanzadeh, S., Jameie, S. B., Mehdizadeh, M., Soleimani, M., Namjoo, Z., & Soleimani, M. (2018). FNDC5 expression in Purkinje neurons of adult male rats with acute spinal cord injury following treatment with methylprednisolone. *Neuropeptides, 70,* 16-25. [DOI:10.1016/j.npep.2018.05.002] [PMID]

Hoet, P. H., Brüske-Hohlfeld, I., & Salata, O. V. (2004). Nanoparticles-known and unknown health risks. *Journal of Nanobiotechnology, 2*(1), 12. [DOI:10.1186/1477-3155-2-12] [PMID]

Honardoost, M., Soleimanjahi, H., & Rajaei, F. (2013). [Apoptosis: Programmed cell death (Persian)]. *Journal of Inflammatory Disease, 17*(3), 48-57. [Link]

Janzadeh, A., Behroozi, Z., Saliminia, F., Janzadeh, N., Arzani, H., & Tanha, K., et al. (2022). Neurotoxicity of silver nanoparticles in the animal brain: A systematic review and meta-analysis. *Forensic Toxicology, 40*(1), 49-63. [DOI:10.1007/s11419-021-00589-4] [PMID]

Kvitek, O., Havelka, V., Vesely, M., Reznickova, A., & Svorcik, V. (2020). Preparation of alloyed and "core-shell" Au/Ag bimetallic nanostructures on glass substrate by solid state dewetting. *Journal of Alloys and Compounds, 829,* 154627. [DOI:10.1016/j.jallcom.2020.154627]

Macchi, B., Marino-Merlo, F., Nocentini, U., Pisani, V., & Cuzzocrea, S., Grelli, S., et al. (2015). Role of inflammation and apoptosis in multiple sclerosis: comparative analysis between the periphery and the central nervous system. *Journal of Neuroimmunology, 287,* 80-87. [DOI:10.1016/j.jneuroim.2015.08.016] [PMID]

Mertens, J., Oorts, K., Leverett, D., & Arijs, K. (2019). Effects of silver nitrate are a conservative estimate for the effects of silver nanoparticles on algae growth and Daphnia magna reproduction. *Environmental Toxicology and Chemistry, 38*(8), 1701-1713. [DOI:10.1002/etc.4463] [PMID]

Mirsanei, J. S., Nazari, M., Shabani, R., Govahi, A., Eghbali, S., Ajdary, M., & Mehdizadeh, R., et al. (2023). Does gold-silver core-shell nanostructure with alginate coating induce apoptosis in human lymphoblastic tumoral (Jurkat) cell line? *Reports of Biochemistry & Molecular Biology, 12*(2), 233-240. [DOI:10.61186/rbmb.12.2.233] [PMID]

Mohamed, E. M., Kattaia, A. A. A., Abdul-Maksoud, R. S., & Abd El-Baset, S. A. (2020). Cellular, molecular and biochemical impacts of silver nanoparticles on rat cerebellar cortex. *Cells, 10*(1), 7. [DOI:10.3390/cells10010007] [PMID]

Nazari, M., Shabani, R., Ajdary, M., Ashjari, M., Shirazi, R., & Govahi, A., et al. (2023). Effects of Au@ Ag core-shell nanostructure with alginate coating on male reproductive system in mice. *Toxicology Reports, 10,* 104-116. [DOI:10.1016/j.toxrep.2023.01.003] [PMID]

Nejati, M., Tameh, A. A., Vahidinia, Z., & Atlasi, M. A. (2018). Mesenchymal stem cells improve ischemic stroke injury by anti-inflammatory properties in rat model of middle cerebral artery occlusion. *Iranian Red Crescent Medical Journal, 20*(1), e55085. [DOI:10.5812/ircmj.55085]

Nikoletopoulou, V., Markaki, M., Palikaras, K., & Tavernarakis, N. (2013). Crosstalk between apoptosis, necrosis and autophagy. *Biochimica et Biophysica Acta, 1833*(12), 3448–3459. [DOI:10.1016/j.bbamcr.2013.06.001] [PMID]

Oral, O., Oz-Arslan, D., Itah, Z., Naghavi, A., Deveci, R., & Karacali, S., et al. (2012). Cleavage of Atg3 protein by caspase-8 regulates autophagy during receptor-activated cell death. *Apoptosis: An International Journal on Programmed Cell Death, 17*(8), 810–820. [DOI:10.1007/s10495-012-0735-0] [PMID]

Pourheydar, B., Soleimani Asl, S., Azimzadeh, M., Rezaei Moghadam, A., Marzban, A., & Mehdizadeh, M. (2016). Neuroprotective effects of bone marrow mesenchymal stem cells on bilateral common carotid arteries occlusion model of cerebral ischemia in rat. *Behavioural Neurology, 2016,* 2964712. [DOI:10.1155/2016/2964712] [PMID]

Sánchez-López, E., Gomes, D., Esteruelas, G., Bonilla, L., Lopez-Machado, A. L., & Galindo, R., et al. (2020). Metal-based nanoparticles as antimicrobial agents: An overview. *Nanomaterials, 10*(2), 292. [DOI:10.3390/nano10020292] [PMID]

Sofi, M. A., Sunitha, S., Sofi, M. A., Pasha, S. K., & Choi, D. (2022). An overview of antimicrobial and anticancer potential of silver nanoparticles. *Journal of King Saud University-Science, 34*(2), 101791. [Link]

Thakur, M., Gupta, H., Singh, D., Mohanty, I. R., Maheswari, U., & Vanage, G., et al. (2014). Histopathological and ultra structural effects of nanoparticles on rat testis following 90 days (Chronic study) of repeated oral administration. *Journal of Nanobiotechnology, 12,* 42. [DOI:10.1186/s12951-014-0042-8] [PMID]

Trickler, W. J., Lantz, S. M., Murdock, R. C., Schrand, A. M., Robinson, B. L., & Newport, G. D., et al. (2010). Silver nanoparticle induced blood-brain barrier inflammation and increased permeability in primary rat brain microvessel endothelial cells. *Toxicological Sciences: An Official Journal of the Society of Toxicology, 118*(1), 160–170. [DOI:10.1093/toxsci/kfq244] [PMID]

Wei, L., Lu, J., Xu, H., Patel, A., Chen, Z. S., & Chen, G. (2015). Silver nanoparticles: synthesis, properties, and therapeutic applications. *Drug Discovery Today, 20*(5), 595–601. [DOI:10.1016/j.drudis.2014.11.014] [PMID]

Xu, L., Shao, A., Zhao, Y., Wang, Z., Zhang, C., & Sun, Y., et al. (2015). Neurotoxicity of silver nanoparticles in rat brain after intragastric exposure. *Journal of Nanoscience and Nanotechnology, 15*(6), 4215–4223. [DOI:10.1166/jnn.2015.9612] [PMID]

Yin, N., Liu, Q., Liu, J., He, B., Cui, L., & Li, Z., et al. (2013). Silver nanoparticle exposure attenuates the viability of rat cerebellum granule cells through apoptosis coupled to oxidative stress. *Small, 9*(9-10), 1831-1841. [DOI:10.1002/smll.201202732] [PMID]

Yin, N., Zhang, Y., Yun, Z., Liu, Q., Qu, G., & Zhou, Q., et al. (2015). Silver nanoparticle exposure induces rat motor dysfunction through decrease in expression of calcium channel protein in cerebellum. *Toxicology Letters, 237*(2), 112-120. [DOI:10.1016/j.toxlet.2015.06.007] [PMID]

This Page Intentionally Left Blank